Operating temperature windows for fusion reactor structural materials

S.J. Zinkle [a,*], N.M. Ghoniem [b]

[a] *Metals and Ceramics Division, Oak Ridge National Laboratory, P.O. Box 2008, Oak Ridge, TN 37831-6376, USA*
[b] *Mechanical and Aerospace Engineering Department, The University of California at Los Angeles, Los Angeles, CA 90095, USA*

Abstract

A critical analysis is presented of the operating temperature windows for nine candidate fusion reactor structural materials: four reduced-activation structural materials (oxide-dispersion-strengthened and ferritic/martensitic steels containing 8–12%Cr, V–4Cr–4Ti, and SiC/SiC composites), copper-base alloys (CuNiBe), tantalum-base alloys (e.g. Ta–8W–2Hf), niobium alloys (Nb–1Zr), and molybdenum and tungsten alloys. The results are compared with the operating temperature limits for Type 316 austenitic stainless steel. Several factors define the allowable operating temperature window for structural alloys in a fusion reactor. The lower operating temperature limit in all body-centered cubic (BCC) and most face-centered cubic (FCC) alloys is determined by radiation embrittlement (decrease in fracture toughness), which is generally most pronounced for irradiation temperatures below $\sim 0.3\, T_M$ where T_M is the melting temperature. The lower operating temperature limit for SiC/SiC composites will likely be determined by radiation-induced thermal conductivity degradation, which becomes more pronounced in ceramics with decreasing temperature. The upper operating temperature limit of structural materials is determined by one of four factors, all of which become more pronounced with increasing exposure time: (1) thermal creep (grain boundary sliding or matrix diffusional creep); (2) high temperature He embrittlement of grain boundaries; (3) cavity swelling (particularly important for SiC and Cu alloys); or (4) coolant compatibility/corrosion issues. In many cases, the upper temperature limit will be determined by coolant corrosion/compatibility rather than by thermal creep or radiation effects. The compatibility of the structural materials with Li, Pb–Li, Sn–Li, He and Flibe (Li_2BeF_4) coolants is summarized. © 2000 Elsevier Science B.V. All rights reserved.

Keywords: Temperature windows; Fusion energy applications; Structural materials

1. Introduction

A wide range of structural materials have been considered over the past 25–30 years for fusion energy applications. This list includes conventional materials (e.g. austenitic stainless steel), low-activation structural materials (ferritic-martensitic steel, V–4Cr–4Ti, and SiC/SiC com-

* Corresponding author. Tel.: + 1-865-5767220; fax: + 1-865-2413650.
E-mail address: zinklesj@ornl.gov1 (S.J. Zinkle).

posites), oxide dispersion strengthened (ODS) ferritic steel, conventional high temperature refractory alloys (Nb, Ta, Cr, Mo, W alloys), titanium alloys, Ni-based super alloys, ordered intermetallics (TiAl, Fe_3Al, etc.), high-strength, high-conductivity copper alloys, and various composite materials (C/C, metal-matrix composites, etc.). Numerous factors must be considered in the selection of structural materials, including

- material availability, cost, fabricability, joining technology
- unirradiated mechanical and thermophysical properties
- radiation effects (degradation of properties)
- chemical compatibility and corrosion issues
- safety and waste disposal aspects (decay heat, etc.)
- nuclear properties (impact on tritium breeding ratio, solute burnup, etc.)

The present paper summarizes current information on the first four items in this list for nine different candidate structural materials, with an emphasis on how these issues impact allowable operating temperature limits. Several of the parameters are compared with austenitic stainless steel, which has a well-developed property database but suffers from relatively low thermal conductivity. Due to the importance of low long-term induced radioactivity of the fusion reactor structure, strong emphasis has been placed within the past 10–15 years on the development of three reduced-activation structural materials: ferritic/martensitic steel containing 8–12%Cr, vanadium-base alloys (e.g. V–4Cr–4Ti), and SiC/SiC composites. Recently there also has been increasing interest in reduced-activation ODS ferritic steels. Additional alloys of interest for fusion applications include copper alloys (CuCrZr, CuNiBe, dispersion-strengthened copper), tantalum-base alloys (e.g. Ta–8W–2Hf), niobium alloys (Nb–1Zr), and chromium, molybdenum and tungsten alloys. Chromium alloys have been excluded from the present survey due to limited data on thermomechanical properties (e.g. creep) compared to the other Group VI alloys. Recent work on Cr alloys has been summarized elsewhere [1]. Although explicitly not covered in the present survey, the important issues of safety/waste management and nuclear properties clearly need to be considered in the selection of structural materials for fusion energy applications. For example, there are significant safety [2–4] and waste disposal [2,3] issues associated with the use of Mo and Nb alloys in conventional fusion blanket systems.

It should be stressed that the detailed minimum and maximum operating temperature limits for a given structural material are strongly dependent on the specific reactor design. The operating temperature limits summarized in this paper are based on typical fusion reactor structural material requirements, and may need modification for specific blanket designs. There have been several previous notable analyses which have produced tentative dose-dependent temperature design windows for ferritic-martensitic steels [5,6] and vanadium alloys [5].

2. Material costs and fabrication issues

The costs per unit mass of large quantities of the candidate structural materials in relatively simple product forms (sheet or plate) are summarized in Table 1. Ferritic and austenitic steels are the lowest-price structural materials due to their

Table 1
Current costs for bulk quantities of simple plate products

| Material	Cost per kg
Fe–9Cr steels	≤$5.50 (plate form)
SiC/SiC composites	>$1000 (CVI processing)
	∼$200 (CVR processing of CFCs)
V–4Cr–4Ti	$200 (plate form — average between 1994 and 1996 US fusion program large heats and Wah Chang 1993 'large volume' cost estimate)
CuCrZr, CuNiBe, ODS copper	∼$10
Nb–1Zr	∼$100
Ta, Ta–10W	$300 (sheet form)
Mo	∼$80 (3 mm sheet); ∼$100 for TZM
W	∼$200 (2.3 mm sheet); higher cost for thin sheet
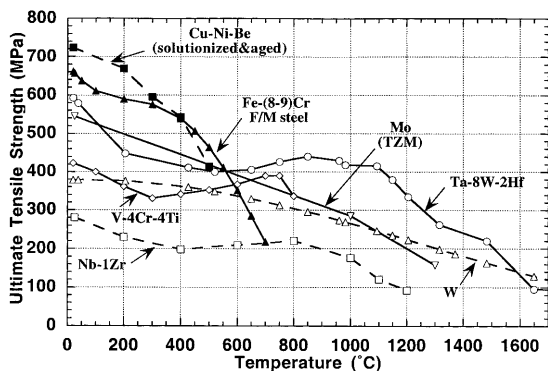
Fig. 1. Comparison of the ultimate tensile strength of recrystallized refractory alloys [10,15–18], solutionized and aged Cu–2%Ni–0.3%Be [19] and Fe–(8–9%)Cr ferritic-martensitic steel [12].

widespread commercial market and relative ease of fabrication. On the other hand, the current standard manufacturing method for producing SiC/SiC composites (chemical vapor infiltration, CVI, of a woven SiC fiber preform) results in very expensive products due to the high cost of fibers and the relatively complicated manufacturing process. Alternative lower cost SiC/SiC infiltration techniques such as reaction bonding or polymer preimpregnation are not included in Table 1 due to the anticipated poor radiation stability of these products. A recent alternative technique for producing high-quality SiC/SiC by chemical vapor reaction (CVR) conversion of carbon-carbon composites [7] is projected to significantly reduce the production costs for SiC/SiC (to levels comparable to refractory alloys). The fabrication costs for producing finished products of refractory alloys (particularly W) are significantly higher than for steels. The Group V refractory metals (V, Nb, Ta) are relatively easy to fabricate into various product forms such as tubing, whereas Group VI refractory metals (Mo, W) are very difficult to fabricate due to their poor ductility at room temperature.

A further issue with SiC/SiC and all refractory metals is joining, particularly in-field repairs. Satisfactory full-penetration welds have not been developed for W, despite intensive efforts over a > 25 year time span (1960–1985). The main issue associated with fusion zone welding of Group V

alloys is the pickup of embrittling interstitial impurities (O, C, N, H) from the atmosphere. Encouraging results have recently been obtained on gas tungsten arc welds of vanadium alloys, although the technique is currently limited to a glovebox controlled atmosphere [8]. One promising alternative joining technique that has recently been developed is friction stir welding [9]. Since friction stir welding is a solid state joining process, the amount of impurity pickup from the surrounding atmosphere is expected to be considerably less than conventional welding techniques (gas tungsten arc, electron beam or laser welding). Friction stir welding may have applications for dispersion strengthened alloys and all of the refractory alloys if appropriate high strength, high temperature stirring tool bits can be developed. An additional potential benefit (yet to be demonstrated) is the possibility of repair-welding irradiated materials containing > 10 appm He.

3. Overview of unirradiated mechanical and thermophysical properties

Recent summaries of the mechanical and physical properties for V–4Cr–4Ti, Fe–8–9Cr martensitic steel, SiC/SiC composites, and T-111 (Ta–8W–2Hf) are published elsewhere [10–13]. A good summary of the properties for W and Type 316 austenitic stainless steel is contained in the International Thermonuclear Experimental Reactor (ITER) Material Properties Handbook (pub. 4 and later versions) [14]. The allowable design stresses of the nine materials considered in this paper is generally controlled by the ultimate strength rather than the yield strength (due to the low work hardening capacity of refractory alloys compared to, e.g. annealed austenitic stainless steel). Fig. 1 shows the unirradiated ultimate tensile strength as a function of temperature for seven different structural alloys [10,12,14–19]. The ultimate strength of SiC/SiC [13] is strongly dependent on the fiber-matrix interfacial layer and weakly dependent on test temperature between 20 and 1000°C. Typical ultimate tensile strengths for SiC/SiC are 220–240 MPa. The ultimate tensile strengths for recrystallized or solution annealed

refractory alloys were used to construct Fig. 1. The tensile strength and ductility of stress-relieved (non-recrystallized) refractory alloys are superior to those of recrystallized specimens, with typical increases in strength of up to a factor of two compared to recrystallized material. However, the possibility of stress- or radiation-enhanced recrystallization of these alloys (along with the likely inclusion of welded joints in the structure) does not allow this strength advantage to be considered for conservative design analyses of fusion reactor structural components.

In addition to the ultimate strength (σ_U), other key properties which determine the resistance to thermal stress are the elastic modulus (E), Poisson's ratio (v), thermal conductivity, (k_{th}), and mean linear coefficient of thermal expansion (α_{th}). A thermal stress figure of merit convenient for qualitative ranking of candidate high heat flux structural materials is given by $M = \sigma_U k_{th}(1-v)/(\alpha_{th}E)$. The maximum allowable heat flux is directly proportional to $M/\Delta x$ (for a constrained flat plate), where Δx is the wall thickness. In addition, temperature limits (usually determined by thermal creep considerations) can be used for additional qualitative ranking of materials. A rigorous quantitative analyses of candidate materials requires the use of advanced structural design criteria such as those developed in the ITER Structural Design Criteria [20].

The thermal stress figure of merit varies from ~ 57 kW/m for a high strength, high conductivity CuNiBe alloy at 200°C [21] to ~ 2.0 for SiC/SiC

at 800°C [13,22] and Type 316 stainless steel at 500°C [14]. However, Cu–Ni–Be is not suitable for structural use above ~ 300°C due to poor fracture toughness at elevated temperature [23,24], and the thermal creep strength of all copper alloys is low at temperatures above 400°C ($0.5T_M$). Therefore, copper alloys are not attractive choices for high thermal efficiency power plants and will be only briefly discussed in the remainder of this paper. The low thermal stress resistance of SiC/SiC is mainly due to the low thermal conductivity in currently available composites (primarily due to a combination of poor quality fibers and imprecise control of the CVI deposition chemistry). The two major classes of low-activation structural alloys, V–Cr–Ti and Fe–8–9Cr martensitic steel have figures of merit of ~ 6.4 (450–700°C) and 5.4 (400°C), respectively. The refractory alloys offer some advantage over vanadium alloys and ferritic-martensitic steel, even in the recrystallized condition. For example, pure recrystallized tungsten has a figure of merit of $M = 11.3$ at 1000°C, and TZM (Mo–0.5Ti–0.1Zr) has a value of $M = 9.6$ at 1000°C. The alloy T-111 (Ta–8W–2Hf) has the best thermal stress figure of merit among the (non-copper) alloys considered, with a value of $M = 12.3$ at 1000°C. Nb–1Zr has an acceptable figure of merit ($M = 10.1$) at 600°C, but its strength and thermal stress capability decrease at temperatures above 600°C. Considering the high induced radioactivity of Nb compared to the other Group V alloys (V and Ta), the lack of a clear thermal stress performance advantage for Nb–1Zr makes this alloy less desirable for fusion energy structural applications compared to the other refractory alloys. Similarly, Mo alloys are less attractive than Cr or W alloys due to safety and waste disposal considerations. However, the mechanical properties database for Cr and W alloys is incomplete.

A major concern for relatively pure W and Mo alloys (e.g. W–2%Re, TZM) is their low fracture toughness even at temperatures above the ductile-to-brittle transition temperature (DBTT). Fig. 2 summarizes the fracture toughness data for pure tungsten in various thermomechanical conditions [25–30]. The limited available data suggest that the fracture toughness is significantly less than
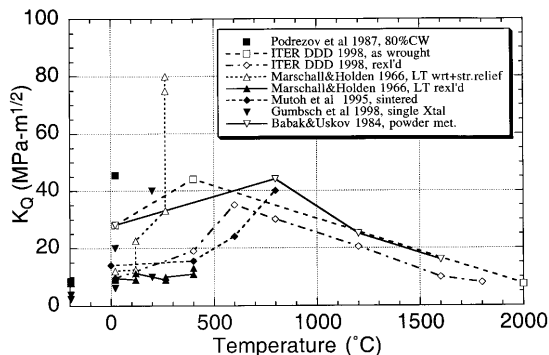

Fig. 2. Temperature-dependent fracture toughness of pure tungsten in various thermomechanical conditions [25–30].

100 MPa-m$^{1/2}$ at all temperatures, with a typical value at 1000°C of ~ 30 MPa-m$^{1/2}$. This is similar to the 'lower-shelf' toughness of irradiated ferritic-martensitic steels and vanadium alloys [31,32]. Addition of 1–2 vol.% of dispersed oxide-particles or Re solute produces a slight increase in the fracture toughness and a shift in the DBTT to lower temperatures [27,28]. The room temperature fracture toughness of tungsten can be increased to ~ 60 to 200 MPa-m$^{1/2}$ by alloying with 3–6% Ni and Fe solute [33,34]. Unirradiated group V refractory alloys such as V–4Cr–4Ti have high fracture toughness (> 100 MPa-m$^{1/2}$) at room temperature [35,36].

4. Lower operating temperature limit for structural materials

The lower temperature limits for the eight remaining types of structural materials (i.e. excluding copper alloys) are strongly influenced by radiation effects. For body-centered cubic (BCC) materials such as ferritic-martensitic steels and the refractory alloys, radiation hardening at low temperatures can lead to a large increase in the ductile to brittle transition temperature [6,37–40]. For SiC/SiC composites, the main concerns at low temperatures are radiation-induced amorphization (with an accompanying volumetric swelling of $\sim 11\%$) [41] and radiation-induced degradation of thermal conductivity.

The radiation hardening in BCC alloys at low temperatures ($< 0.3T_M$) is generally pronounced even for doses as low as ~ 1 dpa [40,42–45]. The amount of radiation hardening typically decreases rapidly with irradiation temperature above $0.3T_M$, and radiation-induced increases in the DBTT may be anticipated to be acceptable at temperatures above $\sim 0.3T_M$ (although experimental verification is needed, particularly for the Mo, W and Ta alloys). Unfortunately, there are very few studies on the mechanical properties of high temperature refractory alloys irradiated and tested at temperatures above $0.3T_M$ (~ 700°C for Mo and W alloys). There are no known fracture toughness measurements on high temperature refractory alloys (Mo, W, Ta alloys) following neutron irradi-

ation at any dose or temperature. The Charpy V-notch impact database on irradiated high temperature refractory alloys is also virtually nonexistent.

The radiation hardening and embrittlement database for ferritic-martensitic steels and V–4Cr–4Ti, Ta, Mo and W alloys is briefly summarized in the following paragraphs. These data were used to make rough estimates of the minimum allowable operating temperature of structural alloys due to radiation embrittlement concerns. A Ludwig–Davidenkov relationship [37,39] between hardening and embrittlement was used to estimate the ductile to brittle transition temperature. In this model, brittle behavior occurs when the temperature dependent stress exceeds the cleavage stress. Due to the lack of fracture mechanics data on irradiated high temperature refractory alloys, the corresponding derived estimates of the minimum allowable operating temperature have relatively high uncertainty (± 100–200°C). It is worth noting that operation at lower temperatures (i.e. within the embrittlement temperature regime) may be allowed for some low-stress fusion structural applications (depending on the value of the operational stress intensity factor relative to the fracture toughness). In addition, it should be noted that the lower-shelf fracture toughness of 'embrittled' ferritic-martensitic steel and V–4Cr–4Ti [31,46,47] is significantly higher than that of unirradiated pure tungsten.

Numerous studies have been performed to determine the radiation hardening and embrittlement behavior of ferritic-martensitic steels. The hardening and DBTT shift are dependent on the detailed composition of the alloy. For example, the radiation resistance of Fe–9Cr–2WVTa alloys appears to be superior (less radiation hardening) to that of Fe–9Cr–1MoVNb [12,32]. The radiation hardening and DBTT shift appear to approach saturation values following low temperature irradiation to doses above 1–5 dpa, although additional high-dose studies are needed to confirm this apparent saturation behavior. At higher doses under fusion conditions, the effects of He bubble accumulation on radiation hardening and DBTT need to be addressed. Based on the
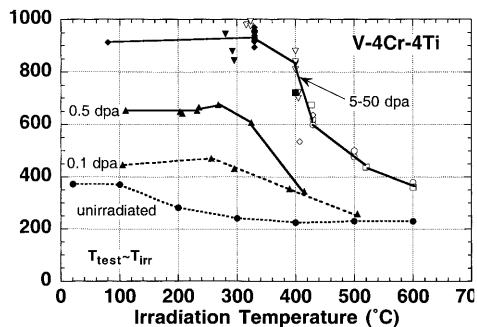
Fig. 3. Effect of irradiation temperature and dose on the yield strength of V–4Cr–4Ti [31,45].

available tensile, Charpy impact and fracture toughness data on fission neutron irradiated ferritic-martensitic steels, the minimum operating temperature that avoids pronounced embrittlement is ~ 200–$250°C$. Recently, some experimental studies have provided evidence that fusion-relevant He generation rates may produce a further increase in the DBTT beyond that attributable to helium hardening effects alone [6,38]. These controversial results were obtained in simulation studies involving He-preimplanted or B- or Ni-doped specimens, which raises the possibility that it might be an artifact associated with the simulation technique. Although useful near-term studies could be performed in 600–800 MeV proton or spallation neutron sources, ultimate resolution of this issue might only be possible when an adequate fusion neutron irradiation facility (e.g. the proposed International Fusion Materials Irradiation Facility [48]) is constructed. If these He-related embrittlement effects are shown to be valid for fusion neutron irradiation conditions, then the minimum operating temperature for ferritic-martensitic steels could be significantly higher than 250°C.

Fig. 3 summarizes the effect of irradiation temperature and dose on the yield strength of V–4Cr–4Ti [31,45]. Pronounced hardening occurs below 400°C ($\sim 0.3T_M$), and an apparent saturation in hardening is reached after a damage level of 1–5 dpa. The hardening is accompanied by a dramatic decrease in the strain hardening capacity, as monitored by uniform elongation tensile data. Corresponding Charpy impact and fracture

toughness investigations have observed brittle behavior ($K_J \sim 30$ MPa-m$^{1/2}$) in V–(4–5)%Cr–(4–5)%Ti specimens irradiated and tested at temperatures $< 400°C$ [31,49]. Only moderate hardening occurs at temperatures above 400–430°C, and radiation embrittlement was not detected in Charpy impact tests of V–(4–5)%Cr–(4–5)%Ti specimens irradiated at 425–600°C for damage levels up to ~ 30 dpa [45]. From a comparison of the yield strength and Charpy impact data of unirradiated and irradiated V–(4–5)%Cr–(4–5)%Ti alloys, brittle fracture occurs when the tensile strength is higher than 700 MPa (the corresponding critical stress for cleavage at a crack tip is actually several times higher than this tensile stress, due to constraint and crack tip geometry considerations). Therefore, 400°C may be adopted as the minimum operating temperature for V–(4–5)%Cr–(4–5)%Ti alloys in fusion reactor structural applications [45]. Further work is needed to assess the impact (if any) of fusion-relevant He generation rates on the radiation hardening and embrittlement behavior of vanadium alloys.

The existing mechanical properties database is very limited for irradiated Nb and Ta alloys (e.g. [50]). Some qualitative trends for Nb and Ta alloys can be inferred from the larger database [45] on irradiated V alloys. Significant radiation hardening has been observed in Ta–(8–10%)W alloys irradiated at 415 and 640°C (tensile strength > 1000 MPa) to a fluence of 1.9×10^{26} n/m^2, $E > 0.1$ MeV, whereas very little hardening occurred at an irradiation temperature of 800°C [50]. This neutron fluence corresponds to a damage level of 2.5 dpa in Ta (10 dpa in steel). Since the matrix hardening in Ta–(8–10%)W at 415 and 640°C is well above the level which produces brittle behavior in V alloys (~ 700 MPa), it is likely that Ta alloys are embrittled at these irradiation conditions (Charpy impact or fracture toughness data are needed to confirm this tentative prediction). Therefore, the minimum operating temperature for Ta–(8–10%)W alloys is estimated to be $\sim 700 \pm 75°C$, based on DBTT considerations.

A moderate mechanical properties database exists for irradiated Mo alloys, although most of the

data were obtained at relatively low irradiation temperatures. Pronounced radiation hardening occurs in Mo and Mo alloys such as TZM and Mo–Re up to $\sim 700°C$. For example, the tensile strength of Mo–5%Re after irradiation at 800°C to a dose of 11 dpa was ~ 1000 MPa for a test temperature of 400°C [51,52]. Very low tensile elongations were observed in Mo, TZM, Mo–Re, and Mo–Zr–B alloys for irradiation and test temperatures up to 700–800°C and damage levels of 5–20 dpa [51,53–55]. Irradiation data at doses > 0.1 dpa are not yet available for the recently-developed Mo–TiC alloys which have been reported to have improved ductility compared to conventional Mo alloys [56]. It is important to note that the impact energy absorption tests carried out to date on these fine-grained Mo–TiC alloys have used smooth (un-notched) specimens. It is difficult to produce a quantitative assessment of the fracture resistance in specimens without a stress concentrator. The estimated minimum operating temperature for Mo alloys is assumed to be $\sim 800 \pm 100°C$, based on the limited tensile data on irradiated specimens. Further mechanical properties data on Mo alloys (in particular Charpy impact or fracture toughness data) at irradiation and test temperatures of 650–950°C are needed to develop a better estimate of the minimum operating temperature associated with DBTT effects.

Very little information is available on the mechanical properties of irradiated W alloys. Tensile elongations of ~ 0 have been obtained for W irradiated at relatively low temperatures of 400 and 500°C ($0.18–0.21T_M$) and fluences of $0.5–1.5 \times 10^{26}$ n/m² (< 2 dpa in tungsten) [50,53,57]. Severe embrittlement (DBTT $> 900°C$) was observed in un-notched bend bars of W and W–10%Re irradiated at 300°C to a fluence of 0.5×10^{26} n/m² (~ 1 dpa) [58]. The rate of embrittlement was found to be most rapid in the W–10%Re alloy. Irradiation data are not yet available for the recently developed fine-grained W–TiC alloy [59] which has been reported to have improved ductility compared to existing W alloys. Since mechanical properties data are not available for pure tungsten or its alloys irradiated at high temperatures, an accurate estimate

of the DBTT versus irradiation temperature cannot be made. The minimum operating temperature which avoids severe radiation hardening embrittlement is expected to be $\sim 900 \pm 100°C$, scaling from the limited Mo alloy data base. Additional data on tungsten and W alloys irradiated at 700–1000°C are clearly needed before a more accurate estimate can be made.

The lower operating temperature limit for SiC/SiC may be due to the $\sim 11\%$ volumetric swelling [41] associated with radiation-induced amorphization or to thermal conductivity degradation issues. Amorphization occurs in SiC at temperatures below $\sim 120°C$ and doses above ~ 1 dpa for fusion reactor-relevant damage rates [41]. This sets a strict lower temperature limit for SiC in structural applications. For high-performance fusion reactor designs [60], the thermal conductivity of SiC/SiC must be maintained above 12–15 W/m-K. Recent advances in SiC processing have resulted in impressive improvements in the thermal conductivity of chemical vapor deposited (CVD) SiC, SiC-based fibers, and SiC/SiC composites. For example, the thermal conductivity of commercially available high-purity CVD SiC exceeds 320 W/m-K at 20°C and 75 W/m-K at 1000°C [13,22], and the thermal conductivity of SiC-based fibers has increased from ~ 3 to 64 W/m-K over the past 10 years [13]. SiC/SiC composites with cross-ply conductivities of ~ 75 W/m-K at 20°C and $\sim 30–35$ W/m-K at 1000°C have recently been fabricated using CVR techniques [7]. However, neutron irradiation causes a pronounced decrease in the thermal conductivity of SiC, particularly at low irradiation temperatures. Most of the degradation occurs below doses of ~ 1 dpa [13,22,61]. Although further data are needed to more accurately establish the dose and temperature dependence, existing data [13,22] and recent results [61] indicate that the thermal conductivity of irradiated SiC/SiC will be less than 10–15 W/m-K for irradiation and test temperatures below $\sim 500°C$. SiC/SiC thermal conductivities higher than 10–15 W/m-K appear to be achievable in advanced composites for irradiation and test temperatures above $\sim 600°C$ [61].

5. Upper operating temperature limit for structural materials

The upper temperature limit for structural materials in fusion reactors may be controlled by four different mechanisms (in addition to safety considerations): Thermal creep, high temperature helium embrittlement, void swelling, and compatibility/corrosion issues. Void swelling is not anticipated to be significant in ferritic-martensitic steel [62] or V–Cr–Ti alloys [63] up to damage levels in excess of 100 dpa, although swelling data with fusion-relevant He/dpa generation rates are needed to confirm this expectation and to determine the lifetime dose associated with void swelling. The existing fission reactor database on high temperature (Mo, W, Ta) refractory alloys (e.g. [50]) indicates low swelling ($< 2\%$) for doses up to 10 dpa or higher. Radiation-enhanced recrystallization (potentially important for stress-relieved Mo and W alloys) and radiation creep effects (due to a lack of data for the refractory alloys and SiC) need to be investigated.

Void swelling is considered to be of particular importance for SiC (and also Cu alloys, which were shown to be unattractive fusion structural materials in Section 3). Fig. 4 summarizes the swelling data for irradiated monolithic SiC [64–67]. Early irradiation studies by Price and coworkers suggested that SiC had negligible
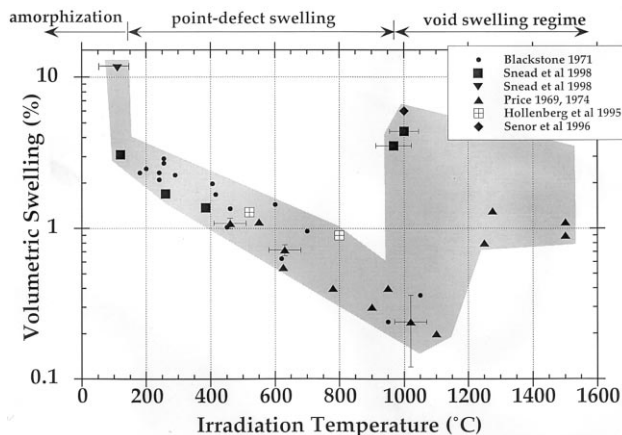

Fig. 4. Volumetric swelling data for irradiated monolithic SiC [64–66].

swelling up to $\sim 1100°C$, and peak void swelling was reported to occur at 1300–1500°C [68]. In contrast, two recent studies have reported significant swelling in SiC-based materials at an irradiation temperature near 1000°C [64,66]. Further work is needed to accurately establish the temperature range for void swelling in SiC. The maximum operating temperature for SiC/SiC due to void swelling concerns is taken to be $990 \pm 40°C$, pending resolution of the apparent conflict between the previous accepted void swelling trend and the two recent studies. Radiation-induced matrix microcracking and strength degradation might impose further limits on this maximum operating temperature, but irradiation data on appropriate advanced SiC/SiC composites are not yet available.

An adequate experimental database exists for thermal creep of ferritic-martensitic steels [69] and the high temperature (Mo, W, Nb, Ta) refractory alloys [16,17,70]. Oxide-dispersion-strengthened ferritic steels offer significantly higher thermal creep resistance compared to ferritic-martensitic steels [71,72], with a steady-state creep rate at 800°C as low as 3×10^{-10} s^{-1} for an applied stress of 140 MPa [72]. The thermal creep behavior of V–4Cr–4Ti is currently being examined in the US [73]. The V–4Cr–4Ti creep data suggest that the upper temperature limit lies between 700 and 750°C, although strengthening effects associated with the pickup of 200–500 ppm oxygen during testing still need to be examined. The thermal creep behavior of SiC/SiC for long exposure times is not well established. However, the predicted thermal creep temperature limit for advanced crystalline SiC-based fibers is above 1000°C [74].

One convenient method to determine the dominant creep process for a given stress and temperature is to construct an Ashby deformation map [75]. Using the established constitutive equations for grain boundary sliding (Coble creep), dislocation creep (power law creep) and self-diffusion (Nabarro–Herring) creep, the dominant deformation-mode regimes can be established. Fig. 5 shows an example of a deformation map for V–4Cr–4Ti, calculated for a creep-relevant deformation rate of 10^{-8} s^{-1} [76]. The calculated map
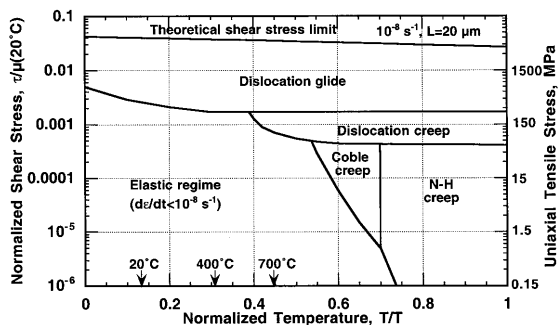
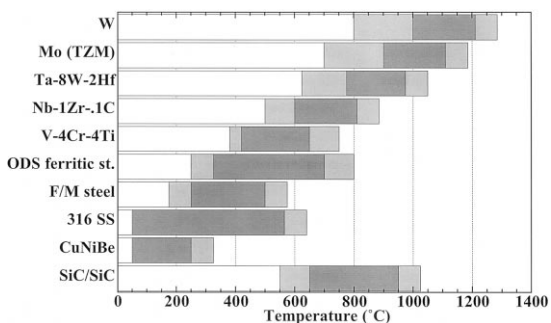Fig. 5. Calculated deformation map for V–4Cr–4Ti [76].

Fig. 6. Operating temperature windows (based on radiation damage and thermal creep considerations) for refractory alloys, Fe–(8–9%)Cr ferritic-martensitic steel, Fe–13%Cr oxide dispersion strengthened ferritic steel, Type 316 austenitic stainless steel, solutionized and aged Cu–2%Ni–0.3%Be, and SiC/SiC composites. The light shaded bands on either side of the dark bands represent the uncertainties in the minimum and maximum temperature limits.

indicates that thermal creep in V–4Cr–4Ti is dominated by dislocation (power law) creep for temperatures between 600 and 850°C, although Coble creep is also exerting some influence. A clear experimental determination of the activation energy for dislocation creep in V–4Cr–4Ti can be readily made at tensile test-relevant strain rates of $\sim 10^{-4}$ s^{-1}, since the calculated deformation map at this strain rate (not shown here, see Ref. [76]) indicates that dislocation creep is the dominant deformation mode over a wide temperature range without any significant influence of Coble creep. As an aside, a similar deformation map analysis for helium embrittlement (which may be considered to be analogous to Coble creep with different activation energies [76]) suggests that

valid data for V–4Cr–4Ti cannot be obtained at tensile test strain rates (10^{-4} s^{-1}). Lower strain rates (10^{-8} s^{-1}) must be used to investigate the susceptibility of V–4Cr–4Ti to helium embrittlement, in agreement with common working knowledge developed from helium embrittlement studies on other alloy systems.

6. Structural material operating temperature windows

Fig. 6 summarizes the operating temperature windows (based on thermal creep and radiation damage considerations) for the nine structural materials considered in this paper. The temperature limits for Type 316 austenitic stainless steel are also included in Fig. 6 for sake of comparison. In this figure, the light shaded regions on either side of the dark horizontal bands are an indication of the uncertainties in the temperature limits. Additional temperature restrictions associated with coolant compatibility issues are summarized in Section 7. Helium embrittlement may cause a reduction in the upper temperature limit, but sufficient data under fusion-relevant conditions are not available for any of the candidate materials. Due to a high density of matrix sinks, ferritic-martensitic steel appears to be very resistant to helium embrittlement [6,77]. An analysis of He diffusion kinetics in vanadium alloys predicted that helium embrittlement would be significant at temperatures $\geq 700°C$ [78]. As discussed in Section 3, the lower temperature limits in Fig. 6 for the refractory alloys and ferritic/martensitic steel are based on fracture toughness embrittlement associated with low temperature neutron irradiation. An arbitrary fracture toughness limit of 30 Mpa-m$^{1/2}$ was used as the criterion for radiation embrittlement. Further work is needed to determine the minimum operating temperature limit for oxide dispersion strengthened (ODS) ferritic steel [6]. The assumed value of $290 \pm 40°C$ used in Fig. 6 was based on results for HT-9 (Fe–12Cr ferritic steel) [47]. The minimum operating temperature for SiC/SiC was based on radiation-induced thermal conductivity degradation, whereas the minimum temperature limit for CuNiBe was

simply chosen to be near room temperature. The low temperature fracture toughness radiation embrittlement is not sufficiently severe to preclude using copper alloys near room temperature [24,79], although there will be a significant reduction in strain hardening capacity as measured by the uniform elongation in a tensile test. The high temperature limit was based on thermal creep for all of the materials except SiC and CuNiBe. Due to a lack of long-term (10 000 h), low-stress creep data for several of the alloy systems, a Stage II creep deformation limit of 1% in 1000 h (3×10^{-9} s^{-1} steady-state creep rate) for an applied stress of 150 MPa was used as an arbitrary criterion for determining the upper temperature limit associated with thermal creep. Further creep data are needed to establish the temperature limits for longer times and lower stresses in several of the candidate materials. As discussed previously, the high temperature limit for SiC was determined by void swelling considerations and the limit for CuNiBe was associated with its low unirradiated fracture toughness at elevated temperatures.

With the exception of CuNiBe, the temperature windows summarized in Fig. 6 are sufficiently wide ($\Delta T = 300$–$400°C$) to enable attractive blanket systems to be designed. The specific values of the operating temperatures need to be combined with compatibility data for the candidate coolants (cf. Section 7) to determine if the temperature window is reduced due to corrosion considerations. One disadvantage with the high minimum operating temperatures of the Ta, Mo and W alloys is that they may require the use of high-performance, high-cost materials (e.g. Ni-based superalloys) in the power conversion piping external to the reactor.

7. Chemical compatibility with coolants

Chemical compatibility issues can reduce the maximum operating temperature for a particular fusion blanket system. Compatibility issues with solid breeder, neutron multiplier and plasma-facing components are not addressed in the present survey and may need to be considered in addition to the gaseous and liquid coolant compatibility limits summarized below.

7.1. Oxidation and impurity pickup

Although oxidation is of concern in all structural materials, the Group VI (Mo, W) alloys are of particular concern due to the formation of volatile (low melting point) oxides which cause significant erosion during exposure to air at temperatures above $\sim 800°C$ [80,81]. Encouraging results on the development of oxidation-resistant refractory alloys (e.g. Mo–6Ti–2.2Si–1.1B [82]) have recently been reported. The effect of temperature and oxygen partial pressure on the erosion rate of Mo and W alloys has been the subject of numerous experimental studies [81,83] and can be modeled by analyzing the thermodynamic and non-equilibrium oxidation behavior [80,81,84]. The experimental studies and theoretical models both show a rapid increase in the erosion rate of Mo and W due to oxidation at temperatures above 1100°C in the presence of low partial pressures of oxygen. The calculated evaporation rate of W and Mo under typical fusion reactor operating conditions (10 MPa helium; 1 ppm oxygen) depends on the importance of boundary layer effects on inhibition of the evaporated oxides in a moving coolant. These conditions have apparently not yet been adequately investigated by experiments. Under laminar flow conditions, the oxygen impingement rate can be significantly lower compared with a static coolant due to the formation of a boundary layer which adds resistance for the impinging oxygen. Initial estimates suggest that the evaporation rate in flowing helium gas may be reduced by several orders of magnitude by this boundary layer [84]. This would reduce the evaporation rate of W and Mo to a level of a few microns per year in 10 MPa of He containing 1 appm oxygen at temperatures up to 1200–1300°C. Experimental confirmation of this predicted effect is needed.

Oxygen, hydrogen and nitrogen pickup in the Group V metals (V, Nb, Ta) causes matrix hardening, which in turn produces an increase in the DBTT. All of the Group V metals have a high oxygen solubility (e.g. 1–3 wt.% oxygen between 20 and 900°C for vanadium). Based on thermodynamic considerations alone, extremely low oxygen partial pressures are required to prevent oxygen

pickup. (e.g. $\ll 10^{-36}$ atm. at $T = 700°C$ [85]). The matrix oxygen concentration in vanadium must be below ~ 1500 wt. ppm to keep the DBTT from rising above room temperature [86,87]. In practice, the oxygen pressure limits for the Group V metals in fusion blanket systems are determined by kinetic rather than thermodynamic considerations. The existence of a protective surface oxide film limits the ingress of oxygen at temperatures below $\sim 600°C$ due to the relatively slow permeation rate of oxygen through the oxide film. For example, the V–4Cr–4Ti activation energy for oxygen diffusion is ~ 130 kJ/mol [88], whereas V–4Cr–4Ti oxide growth has an activation energy of $\sim 180–200$ kJ/mol [89]. However, rapid oxygen pickup occurs at high temperatures in the Group V metals [15]. Therefore, formation of a protective oxide film is not effective at preventing oxygen pickup at the elevated temperatures where these metals would be expected to operate in fusion reactors. Oxygen pickup at temperatures above 600°C can be kept acceptably low (< 1000 wt. ppm within a 3–5 mm thick structure) by limiting the oxygen partial pressure. Assuming an equilibration constant of unity, creation of a monolayer of chemisorbed oxygen on Group V metals at $T > 400°C$ requires ~ 1 Langmuir exposure (10^{-6} torr-s). A simple calculation indicates that 10^{-10} torr is a conservative lower limit for the oxygen partial pressure that would produce an increase in the matrix oxygen

content of 1000 wt. ppm in a 3 mm sheet of any of the Group V metals after long-term (10 years) exposure at high temperatures. Therefore, the upper temperature limit of V, Nb and Ta alloys is $\sim 600°C$ if the oxygen partial pressure in the coolant (e.g. helium) is significantly greater than 10^{-10} torr and there is no oxygen-related temperature limit if the oxygen partial pressure is less than $\sim 10^{-10}$ torr.

7.2. Compatibility with Li, Pb–Li, Sn–Li, and Flibe

The chemical compatibility of the seven remaining structural materials with liquid metals and Flibe (LiF-BeF$_2$ molten salt) is summarized in Table 2 [90–120]. The temperature limits in Table 2 are based on experimental studies of the corrosion of uncoated materials, whereas MHD insulator and/or tritium permeation coatings will clearly be required for many of the structure/coolant combinations listed in the table. Therefore, higher temperature limits than listed in Table 2 might be allowable if self-healing coatings can be successfully developed. Corrosion data for pure tin were used in Table 2 due to the absence of data for Sn–Li. In general, the refractory alloys have very good compatibility with the liquid metals and salts of interest for fusion self-cooled liquid breeder blanket applications. Corrosion associated with impurities in the coolant is one of the

Table 2
Maximum temperatures of structural alloys (bare walls) in contact with high-purity liquid coolants, based on a 5 μm/year corrosion limit [90–120]

	Li	Pb–17 Li	Sn–20Li	Flibe
F/M steel	550–600°C [90–93]	450°C [90,91,93,94]	$\sim 400°C$ [95–97]	700°C? 304/316 SS [98,99]
V alloy	650–700°C [90,100,101]	$\sim 650°C$ [90,102]	?	?
Nb alloy	$\sim 1300°C$ [103–105]	>600°C [102] (>1000°C in Pb) [106]	800°C [106–108]	>800°C [109]
Ta alloy	>1370°C [103,104]	>600°C [102] ($\sim 1000°C$ in Pb) [106]	$\geq 600°C$ [108,110] (<1000°C) [106,107,111]	?
Mo	>1370°C [103,104,112]	>600°C [102]	>700°C [108,110] (<1000°C?) [106,107,110,111,113]	>1100°C? [114,115]
W	>1370°C [103,104]	>600°C [102]	$\sim 1000°C$ [106,108,113]	>900°C in LiF [115]
SiC	<550°C [116–118]	>800°C [118–120]	(>760°C in Sn–Pb–Bi) [120]	?

key engineering issues for refractory alloys in fusion applications.

The Li chemical compatibility data base for high temperature refractory alloys can be summarized as follows: the alloy T-111 (Ta–8W–2Hf) has good compatibility with lithium for exposure temperatures up to 1370°C (both static and circulating loop experiments). Similarly, the existing corrosion data for Nb–1Zr exposed to lithium indicates good compatibility up to 1000°C (static and circulating loops). Pure tungsten and W alloys are generally compatible with lithium up to 1370°C (attack observed at ≥ 1540°C). Mo alloys (TZM) also have good compatibility with lithium up to 1370°C (attack observed at ≥ 1540°C). The compatibility of SiC with Li is uncertain, although thermodynamic analysis [118] and limited experiments [116,117] suggest that pronounced corrosion occurs above ~ 550°C. Polycrystalline SiC of unspecified purity was strongly attacked during exposure to lithium at 815°C for 100 h [119].

The chemical compatibility of Pb–Li and Sn–Li with many of the candidate structural materials is unknown. The corrosion behavior of Pb–Li has been adequately studied only for ferritic-martensitic steel and vanadium alloys. The temperature limit of ferritic-martensitic steel due to Pb–Li corrosion is lower than the thermal creep limit. Due to the chemical incompatibility of iron-base alloys with liquid lead, a corrosion barrier would be required in order to access the high temperature capability of ODS ferritic steels in a Pb–Li cooled system. The limited experimental database on corrosion of structural materials in Sn consists of short-term (< 1000 h) isothermal static tests only. Austenitic and ferritic steels corrode rapidly in Sn at temperatures above ~ 400°C. Additional experimental data on Sn–Li compatibility are needed for other structural materials. The most promising candidates for Sn–Li cooled systems are V alloys and SiC/SiC composites. Mo, W and Ta-base alloys are the least promising structural materials for Sn–Li cooled fusion systems since their respective minimum operating temperatures to avoid radiation embrittlement are comparable to their maximum allowable temperatures associated with Sn–Li corrosion considerations.

The chemical compatibility database for Flibe is even less certain than for the other candidate liquid breeder coolants. The limited data suggest that Flibe may have good compatibility with several of the proposed structural metals (in particular Mo alloys), but data are not yet available for many of the candidate structural materials.

8. Summary and conclusions

The determination of minimum and maximum allowable temperature limits for structural materials (Fig. 6 and Table 2) requires consideration of several factors. In BCC alloys, the minimum operating temperature limit will likely be determined by radiation hardening and embrittlement issues. The minimum temperature limit for SiC/SiC composites will likely be determined by thermal conductivity degradation effects. The upper temperature limit for BCC alloys will typically be determined by either thermal creep, helium embrittlement, or chemical compatibility issues. The upper temperature limit for SiC/SiC will likely be determined by either void swelling or chemical compatibility issues (helium embrittlement and thermal creep would be expected to become pronounced at higher temperatures than the void swelling limit in SiC, which is estimated to occur at ~ 950°C). There are large uncertainties in the allowable temperature window for high temperature refractory alloys due to a lack of mechanical properties tests (fracture toughness, helium embrittlement of grain boundaries) on irradiated material.

Additional issues which need to be considered in the selection of the structural materials include transmutation effects (long term activation and burn-up of alloy elements), afterheat/safety issues (including volatization), and availability/proven resources. In order to perform a more comprehensive analysis of the potential suitability of refractory alloys for fusion structural applications, additional experimental data are needed on chemical compatibility with coolants, fracture toughness before and after irradiation, and on possible joining methods (gas tungsten arc, friction stir welding, etc.) for fabrication of original components and for field repairs.

Acknowledgements

References

[1] H. Stamm, M.R. Bonansinga, F.D.S. Marques, P. Hähner, H. Kolbe, A. Volcan, Thermomechanical characteristics of low activation chromium and chromium alloys, J. Nucl. Mater. 258–263 (1998) 1756–1761.

[2] S.J. Piet, E.T. Cheng, L.J. Porter, Accident safety comparison of elements to define low-activation materials, Fus. Technol. 17 (1990) 636–657.

[3] E.T. Cheng, Concentration limits of natural elements in low activation fusion materials, J. Nucl. Mater. 258–263 (1998) 1767–1772.

[4] G.R. Smolik, D.A. Petti, S.T. Schuetz, Oxidation and volatilization of TZM alloy in air, J. Nucl. Mater., Proc. 9th Int. Conf. Fusion Reactor Materials 2000 (in press).

[5] H. Matsui, et al., Fusion reactor materials selection based on recent progress, Fus. Technol. 30 (1996) 1293–1298.

[6] A. Hishinuma, A. Kohyama, R.L. Klueh, D.S. Gelles, W. Dietz, K. Ehrlich, Current status and future R&D for reduced-activation ferritic/martensitic steels, J. Nucl. Mater. 258–263 (1998) 193–204.

[7] W. Kowbel, K.T. Tsou, J.C. Withers, G.E. Youngblood, High thermal conductivity SiC/SiC composites for fusion applications-II, in Fusion Materials Semiann. Prog Rep. for period ending Dec. 31 1997, DOE/ER-0313/23, Oak Ridge National Lab, 1997, pp. 172–174.

[8] M.L. Grossbeck, J.F. King, Impurity effects on gas tungsten arc welds in V–Cr–Ti alloys, J. Nucl. Mater., Proc. 9th Int. Conf. Fusion Reactor Materials 2000 (in press).

[9] A. Sanderson, Advanced welding techniques for fusion device, Fus. Eng. Design., Proc. 5th Int. Symp. Fusion Nuclear Technology, Rome (1999) submitted.

[10] S.J. Zinkle, Thermophysical and mechanical properties of V–(4–5%)Cr–(4–5%)Ti alloys, in Fusion Materials Semiann. Prog. Report for period ending Dec. 31 1997, DOE/ER-0313/23, Oak Ridge National Lab, 1997, pp. 99–108.

[11] S.J. Zinkle, A.F. Rowcliffe, C.O. Stevens, High temperature tensile properties of V–4Cr–4Ti, in Fusion Materials Semiann. Prog. Report for period ending June 30

1998, DOE/ER-0313/24, Oak Ridge National Lab, 1998, pp. 11–14.

[12] S.J. Zinkle, J.P. Robertson, R.L. Klueh, Thermophysical and mechanical properties of Fe–(8–9%)Cr reduced activation steels, in Fusion Materials Semiann. Prog. Report for period ending June 30 1998, DOE/ER-0313/24, Oak Ridge National Lab, 1998, pp. 135–143.

[13] S.J. Zinkle, L.L. Snead, Thermophysical and mechanical properties of SiC/SiC composites, in Fusion Materials Semiann. Prog. Report for period ending June 30 1998, DOE/ER-0313/24, Oak Ridge National Lab, 1998, pp. 93–100.

[14] J.W. Davis, ITER Material Properties Handbook, ITER Document No. S74 MA 2 97-12-12 R 0.2, 4th edition, 1997.

[15] T.E. Tietz, J.W. Wilson, Behavior and Properties of Refractory Metals, Stanford University Press, Stanford, CA, 1965.

[16] D.C. Goldberg, Nonferrous alloys, in: W.F. Brown, Jr (Ed.), Aerospace Structural Metals Handbook, AFML-TR 68-115, Metals and Ceramics Information Center, Battelle Columbus Laboratories, USA, 1969.

[17] J.B. Conway, Mechanical and physical properties of refractory metals and alloys, in: R.H. Cooper, Jr., E.E. Hoffman (Eds.), Proc. Symp. on Refractory Alloy Technology for Space Nuclear Power Applications, CONF-8308130, Oak Ridge National Lab, 1984, pp. 252–277.

[18] R.W. Buckman, Jr, Development of high-strength fabricable tantalum-base alloys, in: C.L. Briant, et al. (Eds.), High Temperature Silicides and Refractory Alloys, MRS Symposium Proceedings, vol. 322, Materials Research Society, Pittsburgh, 1994, pp. 329–339.

[19] S.J. Zinkle, W.S. Eatherly, Effect of heat treatments on the tensile and electrical properties of high-strength, high-conductivity copper alloys, in Fusion Materials Semiann. Prog. Report for Period ending June 30, 1997, DOE/ER-0313/22, Oak Ridge National Lab, 1997, pp. 143–148.

[20] S. Majumdar, G. Kalinin, ITER structural design criteria and its extension to advanced fusion reactor blankets, J. Nucl. Mater., Proc. 9th Int. Conf. Fusion Reactor Materials 2000 (in press).

[21] S.J. Zinkle, W.S. Eatherly, Effects of test temperature and strain rate on the tensile properties of high-strength, high-conductivity copper alloys, in Fusion Materials Semiann. Prog. Report for Period ending Dec. 31, 1996, DOE/ER-0313/21, Oak Ridge National Lab, 1996, pp. 165–174.

[22] S.J. Zinkle, L.L. Snead, Materials research and development for fusion energy applications, in: P. Vincenzini (Ed.) 9th CIMT-World Forum on New Materials, Symp. VII-Innovative Materials in Advanced Energy Technologies, Techna Srl, Faenza, Italy, 1999, pp. 307–318.

[23] D.J. Alexander, S.J. Zinkle, A.F. Rowcliffe, Fracture Toughness of Copper-Base Alloys for ITER Applications: A Preliminary Report, in Fusion Materials Semi-

ann. Prog. Report for Period ending Dec. 31, 1996, DOE/ER-0313/21, Oak Ridge National Lab, 1996, pp. 175–182.

[24] D.J. Alexander, S.J. Zinkle, A.F. Rowcliffe, Fracture toughness of copper-base alloys for fusion energy applications, J. Nucl. Mater. 271&272 (1999) 429–434.

[25] C.W. Marshall, F.C. Holden, Fracture toughness of refractory metals and alloys, in: R.W. Fountain, et al. (Eds.), High Temperature Refractory Metals: Metallurgical Society Conf. 34, Gordon & Breach, New York, 1966, pp. 129–159.

[26] A.V. Babak, E.I. Uskov, Methodological aspects of studying the fracture toughness of tungsten. 2, Strength Mater. 16 (1984) 943–949.

[27] Y.N. Podrezov, O.G. Radchenko, N.G. Danilenko, V.V. Panichkina, V.I. Gachegov, O.B. Ol'shanskii, Mechanical properties and structure of tungsten-rhenium powder metallurgy deformed alloys, Soviet Powder Metall. Met. Ceram. 26 (1987) 677–680.

[28] Y. Mutoh, K. Ichikawa, K. Nagata, M. Takeuchi, Effect of rhenium addition on fracture toughness of tungsten at elevated temperatures, J. Mater. Sci. 30 (1995) 770–775.

[29] P. Gumbsch, J. Riedle, A. Hartmaier, H.F. Fischmeister, Controlling factors for the brittle-to-ductile transition in tungsten single crystals, Science 282 (1998) 1293–1295.

[30] V.R. Barabash, in ITER Materials Assessment Report, ITER Document No. G A1 DDD 01 97-08-13 W0.1, 1998.

[31] S.J. Zinkle, L.L. Snead, A.F. Rowcliffe, D.J. Alexander, L.T. Gibson, Effect of irradiation temperature and strain rate on the mechanical properties of V–4Cr–4Ti irradiated to low doses in fission reactors, in Fusion Materials Semiann. Prog. Report for period ending June 30 1998, DOE/ER-0313/24, Oak Ridge National Lab, 1998, pp. 33–40.

[32] J.P. Robertson, R.L. Klueh, K. Shiba and A.F. Rowcliffe, Radiation hardening and deformation behavior of irradiated ferritic-martensitic Cr-steels, in Fusion Materials Semiann. Prog. Report for period ending Dec. 31 1997, DOE/ER-0313/23, Oak Ridge National Lab, 1997, pp. 179–187.

[33] K.M. Ostolaza Zamora, J. Gil Sevillano, M. Fuentes Perez, Fracture toughness of W heavy metal alloys, Mater. Sci. Eng. A157 (1992) 151–160.

[34] J.H. Underwood, F.I. Baratta, J.J. Zalinka, Fracture toughness tests and displacement and crack-stability analyses of tungsten round bend specimens, Exp. Mech. 31 (1991) 353–359.

[35] R.J. Kurtz, M.L. Hamilton, H. Li, Grain boundary chemistry and heat treatment effects on the ductile-to-brittle transition behavior of vanadium alloys, J. Nucl. Mater. 258–263 (1998) 1375–1379.

[36] E. Donahue, G.R. Odette and G.E. Lucas, Effect of orientation on effective toughness-temperature curves in V–4Cr–4Ti, in Fusion Materials Semiann. Prog. Report for period ending June 30 1999, DOE/ER-0313/26, Oak Ridge National Lab, 1998, pp. 33–35.

[37] B.L. Cox, F.W. Wiffen, The ductility in bending of molybdenum alloys irradiated between 425 and 1000°C, J. Nucl. Mater. 85&86 (1973) 901–905.

[38] R.L. Klueh, D.J. Alexander, Embrittlement of Cr–Mo steels after low fluence irradiation in HFIR, J. Nucl. Mater. 218 (1995) 151–160.

[39] G.R. Odette, G.E. Lucas, Analysis of cleavage fracture potential of martensitic stainless steel fusion structures, J. Nucl. Mater. 117 (1983) 264–275.

[40] M. Rieth, B. Dafferner, H.-D. Röhrig, Embrittlement behaviour of different international low activation alloys after neutron irradiation, J. Nucl. Mater. 258–263 (1998) 1147–1152.

[41] L.L. Snead, S.J. Zinkle, J.C. Hay, M.C. Osborne, Amorphization of SiC under ion and neutron irradiation, Nucl. Instr. Methods B 141 (1998) 123–132.

[42] F.W. Wiffen, The tensile properties of fast reactor neutron irradiated BCC metals and alloys, in: R.J. Arsenault (Ed.), Proc. Int. Conf. on Defects and Defect Clusters in BCC Metals and Their Alloys, Nuclear Metallurgy Vol. 18, National Bureau of Standards, Gaithersburg, MD, 1973, pp. 176–196.

[43] O.P. Maksimkin, Radiation and radiation-anneal hardening of tantalum, Phys. Met. Metallogr. 80 (1995) 592–594.

[44] L.L. Snead, S.J. Zinkle, D.J. Alexander, A.F. Rowcliffe, J.P. Robertson, W.S. Eatherly, Temperature dependence of the tensile and impact properties of V–4Cr–4Ti irradiated to low neutron doses, in Fusion Materials Semiann. Prog. Report for period ending Dec. 31 1997, DOE/ER-0313/23, Oak Ridge National Lab, 1997, pp. 81–98.

[45] S.J. Zinkle, et al., Research and development on vanadium alloys for fusion applications, J. Nucl. Mater. 258–263 (1998) 205–214.

[46] E. Donahue, G.R. Odette, G.E. Lucas, J.W. Sheckherd, A.F. Rowcliffe, Effect of irradiation on toughness-temperature curves in V–4Cr–4Ti, in Fusion Materials Semiann. Prog. Report for period ending Dec. 31 1998, DOE/ER-0313/25, Oak Ridge National Lab, 1998, pp. 32–41.

[47] A.F. Rowcliffe, et al., Fracture toughness and tensile behavior of ferritic-martensitic steels irradiated at low temperatures, J. Nucl. Mater. 258–263 (1998) 1275–1279.

[48] T. Kondo, IFMIF, its facility concept and technology, J. Nucl. Mater. 258–263 (1998) 47–55.

[49] E.E. Gruber, T.M. Galvin, O.K. Chopra, Effects of irradiation to 4 dpa at 390°C on the fracture toughness of vanadium alloys, in Fusion Materials Semiann. Prog. Report for period ending June 30 1998, DOE/ER-0313/24, Oak Ridge National Lab, 1998, pp. 28–32.

[50] F.W. Wiffen, Effects of irradiation on properties of refractory alloys with emphasis on space power reactor applications, in: R.H. Cooper, Jr. and E.E. Hoffman (Eds.), Proc. Symp. on Refractory Alloy Technology for Space Nuclear Power Applications, CONF-8308130, Oak Ridge National Lab, 1984, pp. 252–277.

[51] A. Hasegawa, K. Abe, M. Satou, C. Namba, Tensile behavior and microstructure of neutron-irradiated Mo–5%Re alloy, J. Nucl. Mater. 225 (1995) 259–266.

[52] A. Hasegawa, K. Ueda, M. Satou, K. Abe, Neutron irradiation embrittlement of molybdenum rhenium alloys and their improvement by heat treatment, J. Nucl. Mater. 258–263 (1998) 902–906.

[53] J.M. Steichen, Tensile properties of neutron irradiated TZM and tungsten, J. Nucl. Mater. 60 (1976) 13–19.

[54] V. Chakin, V. Kazakov, Radiation embrittlement of low-alloyed Mo alloys, J. Nucl. Mater. 233–237 (1996) 902–906.

[55] S.A. Fabritsiev, A.S. Pokrovsky, The effect of rhenium on the radiation damage resistivity of Mo–Re alloys, J. Nucl. Mater. 252 (1998) 216–227.

[56] H. Kurishita, Y. Kitsunai, T. Shibayama, H. Kayano, Y. Hiraoka, Development of Mo alloys with improved resistance to embrittlement by recrystallization and irradiation, J. Nucl. Mater. 233–237 (1996) 557–564.

[57] I.V. Gorynin, et al., Effects of neutron irradiation on properties of refractory metals, J. Nucl. Mater. 191–194 (1992) 421–425.

[58] P. Krautwasser, H. Derz, E. Kny, Influence of fast neutron fluence on the DBTT of tungsten, W–10Re and W–3.4Ni–1.6Fe, High Temperatures-High Pressures 22 (1976) 25–32.

[59] Y. Kitsunai, H. Kurishita, H. Kayano, Y. Hiraoka, T. Igarashi, T. Takida, Microstructure and impact properties of ultra-fine grained tungsten alloys dispersed with TiC, J. Nucl. Mater. 271&272 (1999) 423–428.

[60] P. Fenici, A.J. Frias Rebelo, R.H. Jones, A. Kohyama, L.L. Snead, Current status of SiC/SiC composites R&D, J. Nucl. Mater. 258–263 (1998) 215–225.

[61] L.L. Snead, R. Heidinger, Effects of neutron irradiation on the physical properties of ceramics, J. Nucl. Mater., Proc. 9th Int. Conf. Fusion Reactor Materials (1999).

[62] D.S. Gelles, Microstructural examination of commercial ferritic alloys at 200 dpa, J. Nucl. Mater. 233–237 (1996) 293–298.

[63] B.A. Loomis, D.L. Smith, Vanadium alloys for structural applications in fusion systems: a review of vanadium alloy mechanical and physical properties, J. Nucl. Mater. 191–194 (1992) 84–91.

[64] L.L. Snead, et al., Low dose irradiation performance of SiC interphase SiC/SiC composites, J. Nucl. Mater. 253 (1998) 20–30.

[65] G.W. Hollenberg, et al., The effect of irradiation on the stability and properties of monolithic silicon carbide and SiCf/SiC composites up to 25 dpa, J. Nucl. Mater. 219 (1995) 70–86.

[66] D.J. Senor, G.E. Youngblood, J.L. Brimhall, D.J. Trimble, G.A. Newsome, J.J. Woods, Dimensional stability and strength of neutron-irradiated SiC-based fibers, Fus. Technol. 30 (1996) 956–968.

[67] H. Huang, N.M. Ghoniem, A swelling model for stoichiometric SiC at temperatures below 1000°C under neutron irradiation, J. Nucl. Mater. 250 (1997) 192–199.

[68] R.J. Price, Properties of silicon carbide for nuclear fuel particle coatings, Nucl. Tech. 35 (1977) 320–336.

[69] K. Shiba, A. Hishinuma, A. Tohyama, K. Masamura, Properties of Low Activation Ferritic Steel F82H IEA Heat-Interim Report of IEA Round-Robin Tests (1), Japan Atomic Energy Research Institute Report JAERI-Tech 97-038, 1997.

[70] H.E. McCoy, Creep properties of selected refractory alloys for potential space nuclear power applications, Oak Ridge National Lab Report ORNL/TM-10127, 1986.

[71] S. Ukai, T. Nishida, T. Okuda, T. Yoshitake, R&D of oxide dispersion strengthened ferritic/martensitic steels for LMFBR, J. Nucl. Mater. 258–263 (1998) 1745–1749.

[72] P.J. Maziasz et al., New ODS ferritic alloys with dramatically improved high-temperature strength, J. Nucl. Mater., Proc. 9th Int. Conf. Fusion Reactor Materials (1999).

[73] R.J. Kurtz, M.L. Hamilton, Biaxial thermal creep of V–4Cr–4Ti at 700°C and 800°C, in Fusion Materials Semiann. Prog. Report for period ending June 30 1999, DOE/ER-0313/26, Oak Ridge National Lab, 1999, pp. 3–10.

[74] G.E. Youngblood, R.H. Jones, G.N. Morscher, A. Kohyama, Creep behavior for advanced polycrystalline SiC fibers, in Fusion Materials Semiann. Prog. Report for period ending June 30 1997, DOE/ER-0313/22, Oak Ridge National Lab, 1997, pp. 81–86.

[75] M.F. Ashby, A first report on deformation-mechanism maps, Acta Metall. 20 (1972) 887–897.

[76] S.J. Zinkle, G.E. Lucas, Deformation and Fracture Mechanisms in Irradiated FCC and BCC Metals, Workshop on Basic Aspects of Differences in Irradiation Effects between FCC, BCC and HCP Metals and Alloys, Cangas de Onis, Spain, Oct. 15–20, 1998; to be submitted to J. Nucl. Mater. (2000).

[77] H. Schroeder, H. Ullmaier, Helium and hydrogen effects on the embrittlement of iron- and nickel-based alloys, J. Nucl. Mater. 179–181 (1991) 118–124.

[78] A.I. Ryazanov, V.M. Manichev, W. van Witzenburg, Influence of helium and impurities on the tensile properties of irradiated vanadium alloys, J. Nucl. Mater. 227 (1996) 304–311.

[79] S. Tähtinen, M. Pyykkönen, P. Karjalainen-Roikonen, B.N. Singh, P. Toft, Effect of neutron irradiation on fracture toughness behavior of copper alloys, J. Nucl. Mater. 258–263 (1998) 1010–1014.

[80] J.C. Batty, R.E. Stickney, Quasi-equilibrium treatment of gas–solid reactions, part I, J. Chem. Phys. 51 (1969) 4475.

[81] H.A. Jehn, K.K. Schulze, High-temperature gas–metal reactions of molybdenum and its alloys, in: K.H. Miska, et al. (Eds.), Physical Metallurgy and Technology of Molybdenum and its Alloys, AMAX Specialty Metals Corp, Greenwich, CT, 1985, pp. 107–117.

[82] J.A. Shields, Jr, E.L. Baker, Molybdenum alloys and emerging applications (Refractory metals forum), Adv. Mater. Process. 1/99 (1999) 61–64.

[83] P.O. Schissel, O.C. Trulson, J. Chem. Phys. 43 (1965) 737.

[84] S. Sharafat, N.M. Ghoniem, unpublished research (1999).

[85] W.L. Worrell, J. Chipman, A thermodynamic analysis of the Ta–C–O, Cb–C–O and V–C–O systems, in: W.A. Krivsky (Ed.), High Temperature Refractory Metals: Metallurgical Society Conf. 34, Part I, Gordon & Breach, New York, 1965, pp. 335–345.

[86] B.A. Loomis, O.N. Carlson, Investigation of the brittle–ductile transition in vanadium, in: W.R. Clough (Ed.), Reactive Metals, Interscience, London, 1959, pp. 227–243.

[87] B.A. Pint, P.M. Rice, L.D. Chitwood, J.H. DeVan, J.R. DiStefano, Microstructural characterization of external and internal oxide products on V–4Cr–4Ti, in Fusion Materials Semiann. Prog. Report for period ending June 30 1998, DOE/ER-0313/24, Oak Ridge National Lab, 1998, pp. 77–81.

[88] H. Nakajima, S. Nagata, H. Matsui, S. Yamaguchi, Diffusion of oxygen in vanadium and its alloys, Philos. Mag. A 67 (1993) 557–571.

[89] M. Uz, K. Natesan, V.B. Hang, Oxidation kinetics and microstructure of V–(4–5) wt% Cr–(4–5) wt% Ti alloys exposed to air at 300–650°C, J. Nucl. Mater. 245 (1997) 191–200.

[90] S. Malang, R. Mattas, Comparison of lithium and the eutectic lead–lithium alloy, two candidate liquid metal breeder materials for self-cooled blankets, Fus. Eng. Des. 27 (1995) 399–406.

[91] O.K. Chopra, D.L. Smith, Compatibility of ferritic steels in forced circulation lithium and Pb–17Li systems, J. Nucl. Mater. 155–157 (1988) 715–721.

[92] P.F. Tortorelli, Corrosion of ferritic steels by molten lithium: influence of competing thermal mass transfer and surface product reactions, J. Nucl. Mater. 155–157 (1988) 722–727.

[93] P.F. Tortorelli, Dissolution kinetics of steels exposed in lead–lithium and lithium environments, J. Nucl. Mater. 191–194 (1992) 965–969.

[94] M. Broc, T. Flament, P. Fauvet, J. Sannier, Corrosion of austenitic and martensitic stainless steels in flowing 17Li–83Pb alloy, J. Nucl. Mater. 155–157 (1988) 715–721.

[95] L.R. Kelman et al., Argonne National Laboratory, Argonne, IL Report ANL–4417, 1950.

[96] R.N. Lyon (Ed.), Liquid metals handbook, 2nd Edition, US Office of Naval Research, 1952.

[97] B.D. Craig, D.S. Anderson (Eds.), ASM Handbook of corrosion data, 2nd Edition, ASM International, Materials Park, OH, 1995.

[98] J.R. DiStefano, J.H. DeVan, J.R. Keiser, R.L. Klueh, W.P. Eatherly, Materials considerations for molten salt accelerator-based plutonium conversion systems, Oak Ridge National Lab Report ORNL/TM-12925/R1, 1995.

[99] J.R. Keiser, J.H. DeVan, E.J. Lawrence, Compatibility of molten salts with type 316 stainless steel and lithium, J. Nucl. Mater. 85&86 (1979) 295–298.

[100] K. Natesan, C.B. Reed, R. Mattas, Assessment of alkali metal coolants for the ITER blanket, Fus. Eng. Des. 27 (1995) 457–466.

[101] O.K. Chopra, D.L. Smith, Corrosion behavior of vanadium alloys in flowing lithium, J. Nucl. Mater. 155–157 (1988) 683–689.

[102] H. Feuerstein, H. Gräbner, J. Oschinski, S. Horn, Compatibility of refractory metals and beryllium with molten Pb–Li, J. Nucl. Mater. 233–237 (1996) 1383–1386.

[103] J.H. DeVan, J.R. DiStefano, E.E. Hoffman, Compatibility of refractory alloys with space reactor system coolants and working fluids, In: R.H. Cooper, Jr., E.E. Hoffman (Eds.), Proc. Symp. on Refractory Alloy Technology for Space Nuclear Power Applications, CONF-8308130, Oak Ridge National Lab, 1984, pp. 34–85.

[104] J.R. DiStefano, Review of alkali metal and refractory alloy compatibility for Rankine cycle applications, J. Mater. Eng. 11 (1989) 215–225.

[105] J. Saito, S. Inoue, S. Kano, T. Yuzawa, M. Furui, M. Morinaga, Alloying effects on the corrosion behavior of binary Nb-based and Mo-based alloys in liquid Li, J. Nucl. Mater. 264 (1999) 216–227.

[106] H. Shimotake, N.R. Stalica, J.C. Hesson, Corrosion of refractory metals by liquid bismuth, tin and lead at 1000°C, Trans. Am. Nucl. Soc. 10 (1967) 141–142.

[107] H. Shimotake, J.C. Hesson, Static and dynamic corrosion by tin, bismuth and bismuth–sodium alloy up to 1000°C, Trans. Am. Nucl. Soc. 8 (1965) 413–415.

[108] J.R. Lance, G.A. Kemeny, Trans. Metall. Soc. AIME Trans. Q. ASM 56 (1963) 204–205.

[109] W.D. Manley, et al., Metallurgical problems in molten fluoride systems, in: R. Hurst, R.N. Lyon, C.M. Nicholls (Eds.), Progress in Nuclear Energy, Series IV, vol. 2, Pergamon Press, New York, 1960, pp. 164–176.

[110] F.L. LaQue, H.R. Copson (Eds.), Corrosion resistance of metals and alloys, 2nd Edition, ACS Monograph #158, Reinhold, 1963.

[111] T.A. Coultas, Report NAA-SR-192, 1952.

[112] J. Saito, M. Morinaga, S. Kano, M. Furui, K. Noda, Corrosion behavior of Mo–Re based alloys in liquid Li, J. Nucl. Mater. 264 (1999) 206–215.

[113] E.L. Reed, Stability of refractories in liquid metals, J. Am. Ceram. Soc. 37 (1954) 146–153.

[114] J.W. Koger, A.P. Litman, Compatibility of molybdenum-base alloy TZM with LiF–BeF2–ThF4–UF4 (68–20-11.7–0.3 mole percent) at 1100°C, Oak Ridge National Lab, Oak Ridge, TN Report ORNL-TM-2724, 1969.

[115] Y. Desai, K. Vedula, A.K. Misra, Corrosion of refractory metals in molten LiF, J. Met. 40 (1988) A63.

[116] J.W. Cree, M.F. Amateau, Degradation of silicon carbide by molten lithium, J. Am. Ceram. Soc. 70 (1987) C318–C321.

[117] J.E. Battles, Materials for advanced high temperature secondary batteries, Intern. Mater. Rev. 34 (1989) 1–18.

[118] P. Hubberstey, T. Sample, Thermodynamics of the interactions between liquid breeders and ceramic coating materials, J. Nucl. Mater. 248 (1997) 140–146.

[119] W.H. Cook, Corrosion resistance of various ceramics and cermets to liquid metals, Oak Ridge National Lab, Oak Ridge, TN Report ORNL-2391, 1960.

[120] J.S. Tulenko, G. Schoessow, Nuclear fuel concept for the 21st century, Trans. ANS 75 (1996) 72–73.